Earthquakes and Structures, *Vol. 16, No. 2 (2019) 165-175*
DOI: https://doi.org/10.12989/eas.2019.16.2.165

Summarized IDA curves by the wavelet transform and bees optimization algorithm

Homayoon Shahryari[1], M. Reza Karami*[1] and Alireza A. Chiniforush[2]

[1]*Department of Civil Engineering, K.N. Toosi University of Technology, P.O. Box 15875-4416, Tehran, Iran*
[2]*Centre for Infrastructure Engineering and Safety, School of Civil and Environmental Engineering, University of New South Wales, Sydney, Australia*

(Received October 1, 2016, Revised January 9, 2019, Accepted January 10, 2019)

Abstract. Incremental dynamic analysis (IDA), as an accurate method to evaluate the parameters of structural performance levels, requires many non-linear time history analyses, using a set of ground motion records which are scaled to different intensity levels. Therefore, this method is very computationally demanding. In this study, a new method is presented to estimate the summarized (16%, 50%, and 84% fractiles) IDA curves of a first-mode dominated structure using discrete wavelet transform and bees optimization algorithm. This method reduces the number of required ground motion records for the prediction of the summarized IDA curves. At first, a subset of first list ground motion records is decomposed by means of discrete wavelet transform which have a low dispersion estimating the summarized IDA curves of equivalent SDOF system of the main structure. Then, the bees algorithm optimizes a series of factors for each level of detail coefficients in discrete wavelet transform. The applied factors change the frequency content of original ground motion records which the generated ground motions records can be utilized to reliably estimate the summarized IDA curves of the main structure. At the end, to evaluate the efficiency of the proposed method, the seismic behavior of a typical 3-story special steel moment frame, subjected to a set of twenty ground motion records is compared with this method.

Keywords: discrete wavelet transform; summarized IDA curves; frequency content; performance-based earthquake engineering; bees optimization algorithm

1. Introduction

In performance-based earthquake engineering, accurate estimation of seismic demand and structural capacity are important. There are several methods to determine these parameters such as pushover analysis, non-linear time history analysis, and incremental dynamic analysis (IDA). Performing the IDA requires selecting several appropriate ground motion records which should be scaled to different intensity levels to cover the full range of structural response from elastic behavior to global dynamic instability (Vamvatsikos and Cornell 2002). Therefore, for a large number of ground-motion records and several structural non-linear parameters, IDA will be a time consuming and expensive method. Although dispersion in IDA results is an important factor, it is often more concerned to acquire the summarized IDA curve. In the recent years, many different methods and procedures have emerged to estimate the summarized IDA curve to reduce the computational effort.

Vamvatsikos and Cornell (2005, 2006) estimated 16%, 50% and 84% fractiles IDA curves by a Single Degree of Freedom (SDOF) system equivalent to the objective structure and suggested empirical equations available in SPO2IDA software. Mofid *et al*. (2005) and also Han and Chopra (2006) introduced a new modal IDA based on modal pushover analysis in order to estimate IDA parameters. Zarfam and Mofid (2011) used the modal IDA method to estimate the summarized IDA curves for a reinforced concrete structure. Dolšek and Fajfar (2005) determined the seismic demand for several seismic intensities using the Incremental N2 method to estimate summarized IDA curves of an infilled reinforced concrete structures. Azarbakht and Dolšek (2007, 2011) proposed progressive IDA that a limited number of ground motion records (called precedence list) is selected from the initial collection with two genetic algorithm and simple procedure. The selected ground motion records are used to predict summarized IDA curves for the first mode dominated structures. Eghbali *et al*. (2015) compared the results of two new methods (modal IDA and incremental modal pushover analysis) with results of accurate IDA for two 3-story and 9-story steel moment frames. Perus *et al*. (2015) presented a web-based methodology for prediction the summarized IDA curves. They evaluated the applicability of this method by means of an example of a 4-storey wall-equivalent dual system.

For analyzing earthquake grand motion records, fourier transform was conventionally used to determine the frequency content, however, it did not provide any information about time domain. In other words, fourier transform only processes a signal in the frequency domain and sinusoidal waves are the basic function used for decomposition. In contrary, Wavelet transform (WT) effectively represents a signal in both time and frequency

*Corresponding author, Associate Professor
E-mail: rkarami@kntu.ac.ir

ISSN: 2092-7614 (Print), 2092-7622 (Online)

domain, and the basic function is not limited to the sinusoidal wave and any function (mother wavelet) can be selected based on the original features of the signal (Dremin 2005).

WT is one of the accurate methods to analyze nonstationary signals in both frequency and time domains. WT has been used in various fields such as structural control (Kim and Adeli 2005, Amini *et al*. 2013), structural health monitoring (Tibaduiza *et al*. 2013, Fan *et al*. 2013) damage detection (Ovanesova and Suárez 2004, Xiang and Liang 2012, Solís *et al*. 2013), and generation of artificial ground motion records (Sirca and Adeli 2004, Hancock *et al*. 2006, Ghodrati Amiri *et al*. 2011, 2012, Ghodrati Amiri and Namiranian 2013, Ghodrati Amiri *et al*. 2014).

In this study, an attempt has been made to estimate the summarized IDA curves by modifying the frequency content of a limited number of ground motion records from a suitable list. First, the IDA is performed on an equivalent SDOF system using a set of ground motion records. Then, based on Discrete Wavelet Transform (DWT) and Bees Optimization Algorithm (BOA) the frequency content of the limited number of ground motion records is changed to reduce the difference between the original IDA curves and target summarized IDA curves for SDOF system. Later on, the applicability of proposed method is illustrated using generated ground motion records for an analysis of a 3-story special steel moment resisting frame structure subjected to a set of twenty ground motion records.

2. Discrete wavelet transform

WT is based on the concept of translation and scaling of the mother wavelet function over the limited length of the original signal. By changing the scale of basic function, the local characteristics of a signal are achieved, and by translating this function along the time axis, global characteristics of the signal are categorized (Dremin 2005). DWT decomposes the signal into two groups of coefficients using one low-pass filter and one high-pass filter: Approximations (A) and Details (D), which contain low-frequency components and high-frequency components of the signal, respectively (Politis 2002). The Approximate signal represents the global feature of the signal appropriately due to the domination of lower frequencies. Fig. 1 shows the way of decomposing of a signal with frequency content in the interval [0 Hz, 25 Hz] up to 4 levels using DWT. In this figure, the frequency range of each generated signal was shown. Eq (1) based on Fig. 1 defines that the summation of approximate in four levels and all details equals to the original signal.

$$Signal = A_4 + D_4 + D_3 + D_2 + D_1 \tag{1}$$

Approximate ($A_{j,k}$) and details ($D_{j,k}$) of wavelet transform coefficients are defined as follow

$$A_{j,k} = \int f(t)\Phi_{j,k}(t)dt \tag{2}$$

$$cD_{j,k} = \int f(t)\Psi_{j,k}(t)dt\,, \tag{3}$$

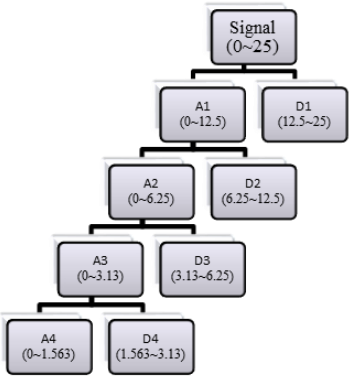

Fig. 1 Decomposing signal to 4 levels by DWT and their frequency range

In both above Equations, Ψ is the mother wavelet function and Φ is scale function of signal $f(t)$ in time domain, j is level of decomposition, and k is an index for that objective coefficient ($A_{j,k}$, $D_{j,k}$). In another hand, to calculate the original signal, inverse DWT (IDWT) is defined as follows

$$f(t) = \sum_{k=-\infty}^{+\infty} A_{j,k}\Phi_{j,k}(t) + \sum_{k=-\infty}^{+\infty} D_{j,k}\Psi_{j,k}(t) \tag{4}$$

To determine the periodic range of detail coefficients at level j of DWT, Eq. (5) is used

$$T_{1j} = 2^j \Delta t\,, \qquad T_{2j} = 2^{j+1}\Delta t \tag{5}$$

where Δt is time step of the signal and the interval [T_{1j}, T_{2j}] is the periodic range of detail coefficients at j^{th} level.

3. Bees optimization algorithm

Swarm-based optimization algorithms mimic nature's methods to drive a search towards the optimal solution. Swarm-based optimization algorithms include the ant colony optimization algorithm (Dorigo *et al*. 1996), the genetic algorithm (Holland 1975) and the particle swarm optimization algorithm (Eberhart and Kennedy 1995). The bees optimization algorithm is inspired by the natural foraging behavior of honey bees to find the optimal solution (Pham and Ghanbarzadeh 2005).

General steps in BOA include: Initialize population with random solutions, evaluate the fitness of each bee (population), choose the bees that have the highest fitness as "selected bees", and sites visited by them are chosen for neighborhood search. Then, recruit bees for selected sites (more bees for best sites) and evaluate fitness values to select the fittest bee from each patch, and assign remaining bees to search randomly to evaluate their fitness. BOA trials terminate when either a maximum number of generations was produced, or a satisfactory fitness level has been reached.

Searches in the neighborhood of the best sites which represent more promising solutions are done in more detail by recruiting more bees for those neighborhoods. One of BOA's drawbacks is the number of utilized adjustable

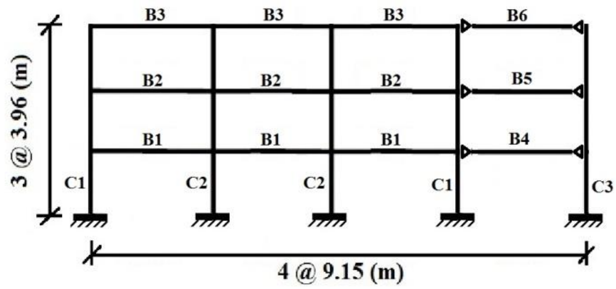

Fig. 2 Geometry of three-story special steel moment resisting frame

Table 1 W-Section used for 3-story structure

column	W-Section	Beam	W-Section	Beam	W-Section
C1	W14x257	B1	W33x118	B4	W18x35
C2	W14x311	B2	W30x116	B5	W18x35
C3	W14x68	B3	W24x68	B6	W16x26

parameters. However, the quantity of the parameter can be determined by conducting a small number of trials. The algorithm is able to converge to the maximum or minimum without being trapped at local optima (Pham and Ghanbarzadeh 2005).

4. Building and ground motions

To evaluate the applicability of the proposed method, a 3-story building as a first-mode dominated structure is assumed to be located in Los Angeles with geometry and properties shown in Fig. 2 and listed in Table 1. Perimeter frames of this structure are special moment frame and internal frames are considered to be gravity frames. A two-dimensional model of the structure is oriented in the north-south direction and is selected from recommended model (M1) at SAC report (Gupta and Krawinkler 1999) which is simulated by Opensees 2.4.0. The yielding strength of columns and beams are 345 MPa and 248 MPa, respectively. Seismic mass of the first and second stories is 478,500 kg and the third story has 520,000 kg mass. The periods of the two first initial modes of the structure are 1.03 and 0.33 seconds. Rayleigh damping method is utilized considering 2% damping ratio for first mode period and 0.2 seconds. For simulation, steel02 fiber element with 3 percent hardening is used (Mazzoni *et al*. 2007) and the first order non-linear geometric $P-\Delta$ effect is considered in structural elements. In addition, the effect of internal gravity frames is simulated by adding an extra gravity column connected to the studied frame and loaded by the half weight of each story. Fig. 3(a) shows the pushover curve based on first mode and idealized pushover curve.

To perform IDA, 20 ground motion records (Table 2) are chosen on the stiff soil with a magnitude of 6.5-6.9, and 15-32 km distance from the source (Vamvatsikos and Cornell 2005). Also, no near-field and directivity effect is considered in the ground motion records. Fig. 3(b) shows IDA curves and summarized fractiles of structure for these ground motion records. Hunt and Fill algorithm (detailed in

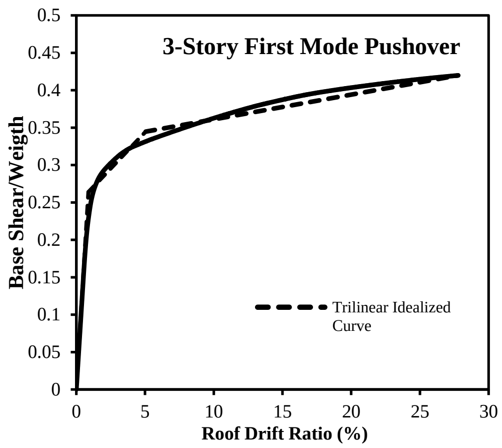

(a) Pushover curve and idealized curve

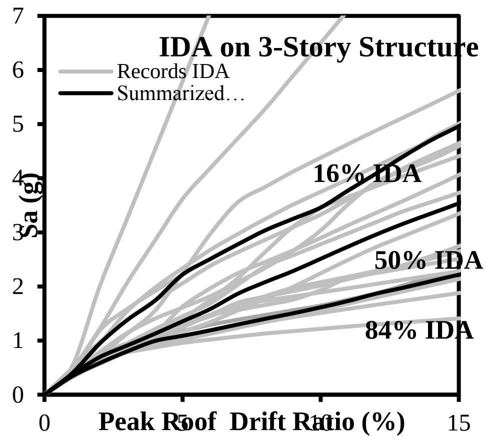

(b) IDA curves with 20 earthquake records and summarized fractiles

Fig. 3 Analyses result on 3-story

Vamvatsikos and Cornell 2004) is used to scale the ground motion records to various level of intensities appropriately. $S_a(T_1,5\%)$ (spectrum acceleration based on first mode of the structure and 5% damping) and peak roof drift ratio are considered as intensity measure (IM) and as damage measure (DM), respectively.

5. Proposed method

The main idea of this paper is to propose a new method to estimate IDA curves of 16%, 50% and 84% fractiles using DWT and BOA. Applying modification in the frequency content of a ground motion record causes changes in response spectrum and IDA curve. For instance, consider Fig. 4(a), acceleration spectrum of Imperial Valley earthquake from Chihuahua station with 5% damping is shown with solid line. Multiplying detail coefficients from one of the levels in DWT by a greater number than 1.0 causes an enhancement of acceleration values on the response spectrum corresponding to the periodic range of the detail coefficients of that level. As shown in Fig. 4(a), if detail coefficients of 6th level of DWT with a periodic range in the interval [0.64 1.28] s are multiplied by 1.5 and 0.5, the spectral acceleration values in this periodic range is

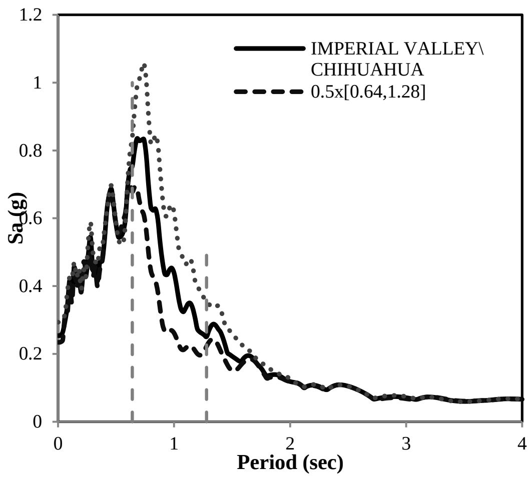

(a) Acceleration spectrum

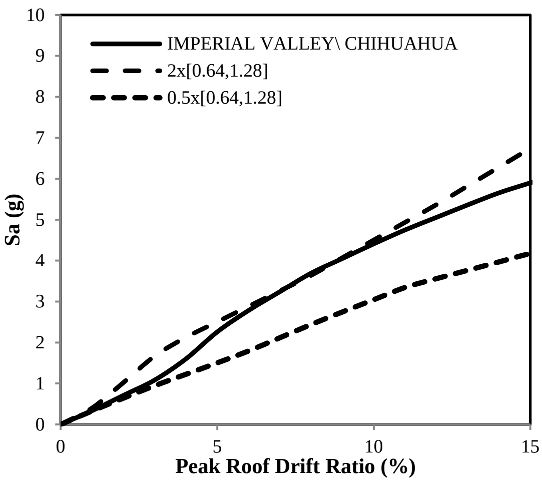

(b) IDA curve

Fig. 4 Effect of change of frequency content

increased and decreased, respectively.

Since multiplying of detail coefficients by a factor change frequency content and $S_a(T,5\%)$ of ground motion record, therefore IDA curve of this new ground motion record will change. As shown in Fig. 4(b), if detail coefficients of 6th level of DWT are multiplied by 2 and 0.5, the IDA curve is moved upward and downward, respectively. This concept will be utilized by means of BOA to optimize change in the frequency content of few ground motion records for better prediction of the summarized IDA curves.

To implement the concept, at the first step, all selected ground motion records should have same time step (Δt=0.02s). Therefore, for the ground motion records with higher resolution (e.g., 0.005s), the additional recorded acceleration data are removed. This procedure can change the resolution of produced ground motion records and consequently the results of non-linear time history analysis and IDA, however, increasing the time step can decrease the entire time of proposed method and is inevitable for its implementation.

In the second step, an equivalent SDOF system of the main structure is determined by means of pushover analysis

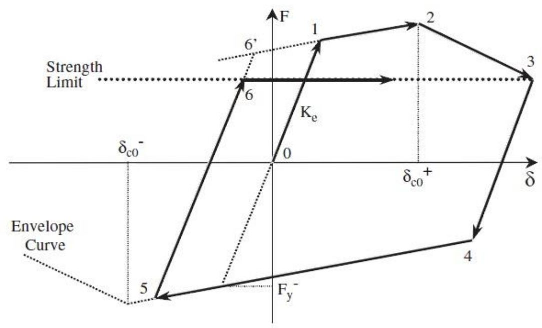

Fig. 5 Bilinear strength limit hysteretic behavior (Ibarra *et al*. 2005)

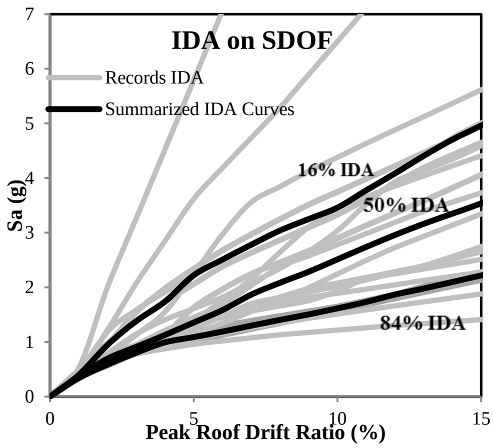

Fig. 6 IDA curves on SDOF system curves with 20 earthquake records and summarized fractiles

(Fajfar 1999). Lateral load distribution (S_n^*) is considered as proportional the first mode, $S_n^* = m\phi_n$ which m is the mass matrix and ϕ_n is the modal shape in n^{th} mode. Then, base shear - roof displacement curve (V_b−u_r) is drawn and idealized as multi-linear curve (Fig. 3(a)). For obtained force-displacement backbone curve (F-D), the value of roof modal shape component is normalized to 1.0. According to the modal shape of the first mode and the mass matrix of the structure, the values of modal effective mass M_n^* (Eq. (6)) and also transformation factor Γ_n (Eq. (7)) are calculated.

Finally to produce backbone curve, the horizontal axis of idealized pushover curve which is roof displacement is divided by Γ_n (D=u_r/Γ_n), and the vertical axis which is base shear is divided by modal effective mass ($F = V_b / M_n^*$).

$$\Gamma_n = \frac{\sum m_i \phi_{in}}{\sum m_i \phi_{in}^2} \qquad (6)$$

$$M_n^* = \frac{\left(\sum_i m_i \phi_{in}\right)^2}{\sum_i m_i \phi_{in}{}^2} \qquad (7)$$

In this case, the main period of SDOF system will be equal to $2\pi\sqrt{D_y/F_y}$ which F_y and D_y are the value of yield force and yield displacement on Backbone curve of

Table 2 List of the ground motion records

No	Record Name	Station	Time	dt (sec)	Distance (km)	Magnitude	Soil (USGS)	Component	PGA (G)
1	IMPERIAL VALLEY	CHIHUAHUA	15/10/1979	0.01	28.7	6.5	C	282	0.254
2	IMPERIAL VALLEY	CUCAPAH	15/10/1979	0.005	23.6	6.5	C	85	0.309
3	IMPERIAL VALLEY	EL CENTRO ARRAY #13	15/10/1979	0.005	21.9	6.5	C	140	0.117
4	IMPERIAL VALLEY	EL CENTRO ARRAY #13	15/10/1979	0.005	21.9	6.5	C	230	0.139
5	IMPERIAL VALLEY	PLASTER CITY 045	15/10/1979	0.005	31.7	6.5	C	135	0.057
6	IMPERIAL VALLEY	PLASTER CITY	15/10/1979	0.005	31.7	6.5	C	45	0.042
7	IMPERIAL VALLEY	WESTMORELAND FIRE STA	15/10/1979	0.005	15.1	6.5	C	90	0.074
8	IMPERIAL VALLEY	WESTMORELAND FIRE STA	15/10/1979	0.005	15.1	6.5	C	180	0.11
9	LOMA PRIETA	SUNNYVALE COLTON AVE	18/10/1989	0.005	28.8	6.9	C	270	0.207
10	LOMA PRIETA	SUNNYVALE COLTON AVE	18/10/1989	0.005	28.8	6.9	C	360	0.209
11	LOMA PRIETA	AGNEWS STATE HOSPITAL	18/10/1989	0.005	28.2	6.9	C	90	0.159
12	LOMA PRIETA	ANDERSON DAM DOWNSTREAM	18/10/1989	0.005	21.4	6.9	B	360	0.24
13	LOMA PRIETA	COYOTE LAKE DAM DOWNST	18/10/1989	0.005	22.3	6.9	B	285	0.179
14	LOMA PRIETA	HOLLISTER DIFF ARRAY	18/10/1989	0.005	25.8	6.9	-	165	0.269
15	LOMA PRIETA	HOLLISTER DIFF ARRAY	18/10/1989	0.005	25.8	6.9	-	255	0.279
16	LOMA PRIETA	HOLLISTER SOUTH & PINE	18/10/1989	0.005	28.8	6.9	-	0	0.371
17	LOMA PRIETA	WAHO	18/10/1989	0.005	16.9	6.9	-	0	0.37
18	LOMA PRIETA	WAHO	18/10/1989	0.005	16.9	6.9	-	90	0.638
19	SUPERSTITION HILLS	WILDLIFE LIQUEFACTION ARRAY	24/11/1987	0.005	24.4	6.7	C	90	0.18
20	SUPERSTITION HILLS	WILDLIFE LIQUEFACTION ARRAY	24/11/1987	0.005	24.4	6.7	C	360	0.2

SDOF system. To allocate hysteretic behavior, different approaches are recommended in literature such as Bilinear Strength Limit (Han and Chopra 2006) and Peak-Oriented and Pinching (Dolšek and Fajfar 2005, Azarbakht and Dolšek 2007). Bilinear Strength Limit is mainly used for steel moment frames and will be utilized herein to run the non-linear dynamic analysis (Fig. 5). In this approach, the unloading point of number 3 (Fig. 5) is considered as the ultimate strength limit, and after point 5, the behavior of system won't extend to point 6′ and terminates at point 6.

In the third step, the IDA is performed using 20 ground motion records on SDOF system. The IDA and summarized curves are illustrated in Fig. 6.

Aim in the fourth step is to reduce the number of ground motion records based on having less difference comparing with target summarized IDA curves. To do so, a criterion is implemented (Eq. (8)) to select the best-fitted records from Table 2

$$IDA\quad Difference = 100 \times \frac{\int_0^{DM_{\max}} \left|\Delta IM_{GR,TS}\, d(DM)\right|}{\int_0^{DM_{\max}} IM_{TS}\, d(DM)} \tag{8}$$

where $\int_0^{DM_{\max}} \left|\Delta IM_{GR,TS}\, d(DM)\right|$ represents the area between IDA curves of selected ground motion record and target summarized IDA curve, $\int_0^{DM_{\max}} IM_{TS}\, d(DM)$ is the area under the target summarized IDA curve when the drift ratio parameter varies between 0 and $DM_{\max}$=0.15. The IDA difference of all ground motion records calculated and three ground motion records with a low difference are selected. The number of selected ground motion record determined based on a procedure described in section 6. In Table 3, for each summarized IDA curve, the IDA difference of the all ground motion records are presented in ascending order.

In the next step, selected ground motion records from Table 3 is decomposed to j level by means of DWT. To get better results, the appropriate number of decomposition levels is determined to have the first mode period of the structure in the periodic range of detail coefficients for $(j\text{-}2)^{\text{th}}$ level of decomposition. Since the time step of all ground motion records were changed to 0.02 s (frequency range of ground motion records are between 0 to 25 Hz), for j=7, the periodic range of detail coefficients (Eq. (5)) in fifth level posses in the interval [0.64 1.28] s which includes the period of first mode for the 3-story structure (T_1=1.03 s).

Table 3 The IDA difference of ground motion records from each summarized IDA curve in ascending order

84% IDA		50% IDA		16% IDA	
Record No.	IDA Difference	Record No.	IDA Difference	Record No.	IDA Difference
19	2.743	20	7.098	16	1.081
4	3.871	13	8.551	3	6.799
9	4.236	5	8.813	2	7.093
10	7.782	11	14.277	15	9.737
14	13.230	14	17.461	6	10.019
8	15.078	10	21.826	1	14.806
11	17.692	12	23.209	12	19.912
13	27.405	19	26.062	20	31.062
5	27.888	4	28.080	5	39.387
7	31.000	9	28.232	13	39.616
20	45.747	8	36.960	11	44.220
12	68.981	6	39.809	14	46.335
6	91.795	15	40.169	10	49.173
15	92.174	3	43.346	19	51.892
3	96.647	7	49.357	4	53.112
2	106.980	2	52.346	9	53.338
16	111.589	16	54.238	8	58.882
1	138.828	1	74.197	7	67.073
18	277.176	18	174.943	18	78.762
17	600.901	17	410.922	17	232.191

Afterward, to modify the frequency content of selected ground motion records according to target summarized IDA curve, a series of modification factors are determined by using BOA. Considering a factor for detail coefficients in each level of DWT and using 7 level of decomposition, the total number of modification factors will be equal to 7. These modification factors are considered as variables of BOA and fitness function for this algorithm is defined by Eq. (8). All procedure of optimization is calculated using IDA of the SDOF system. Table 4 shows the modification factors of three selected ground motion records for each summarized IDA curve according to Table 3.

Table 4 Modification factors for details coefficient of three selected ground motion

IDA Fractiles	IDA 84%			IDA 50%			IDA 16%		
No. Records	19	4	9	20	13	5	16	3	2
DWT level=7	0.737	0.769	0.631	0.803	1.111	1.067	1.073	1.048	1.200
DWT level=6	1.256	1.085	1.029	0.944	0.851	0.736	1.060	1.141	1.001
DWT level=5	1.009	0.408	0.821	0.874	1.013	1.072	1.072	1.178	1.164
DWT level=4	0.660	0.488	0.916	0.957	1.263	0.273	1.012	1.222	0.552
DWT level=3	0.476	1.392	1.442	1.014	0.985	1.113	0.962	1.316	0.842
DWT level=2	1.318	0.869	0.687	1.560	0.637	1.249	1.053	0.960	0.790
DWT level=1	1.015	0.870	1.382	0.844	0.958	0.796	0.957	1.680	0.896

In the seventh step, the modification factors are applied to detail coefficients of DWT and then new ground motion record is regenerated by using IDWT (Eq. (4)). Fig. 7 shows the complete flowchart of suggested method.

In other to evaluate the effect of modification factors on frequency content, the acceleration response spectrum and

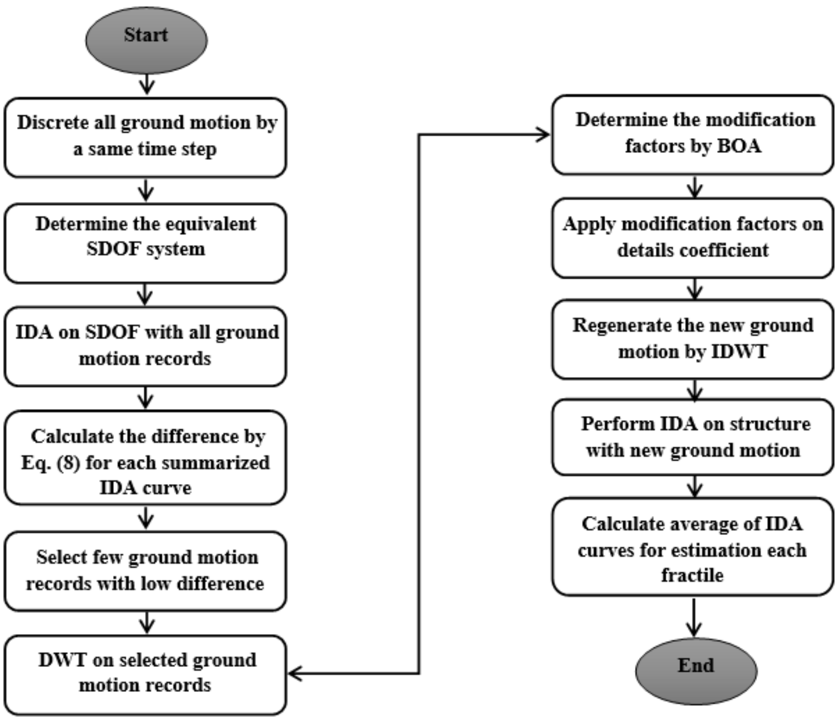

Fig. 7 Complete flowchart of suggested method

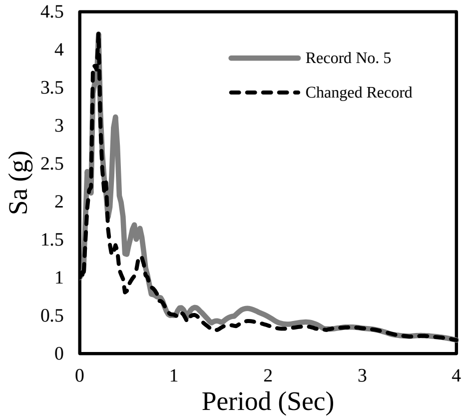

(a) Record No. 5

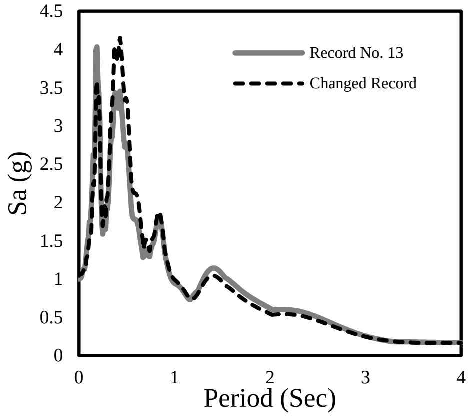

(b) Record No. 13

Fig. 8 Comparison between response spectra of first ground motion records with corresponding generated ground motion records

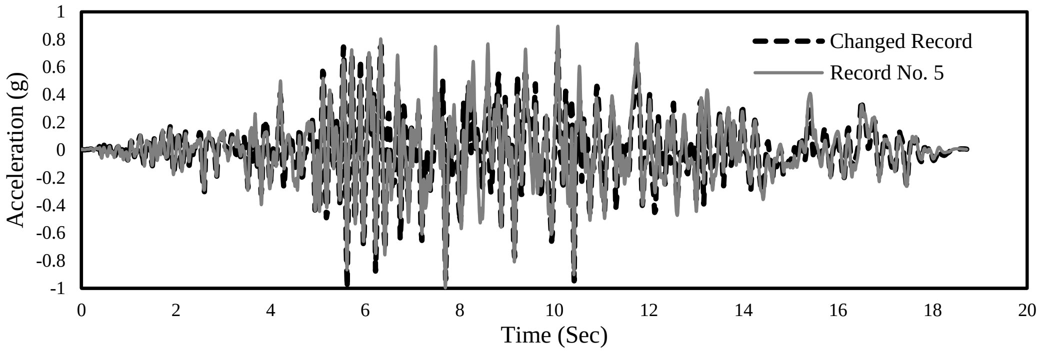

(a) Record No. 5

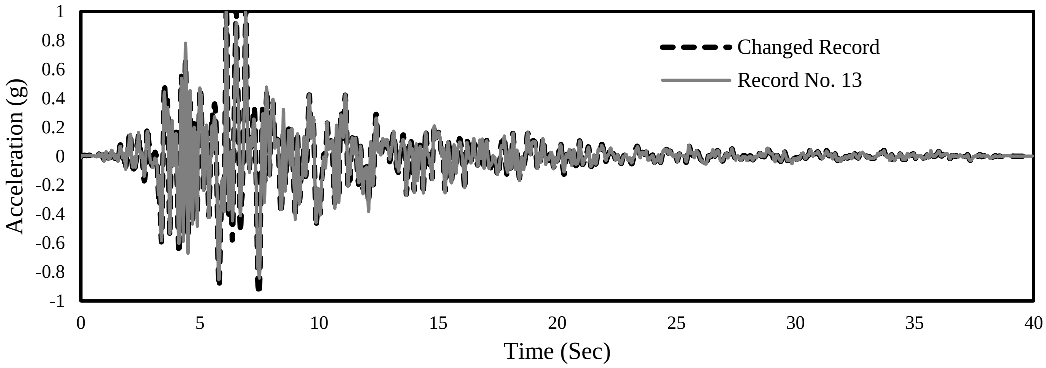

(b) Record No. 13

Fig. 9 Comparison between acceleration time histories of first ground motion records with corresponding generated ground motion records

the time history are drawn in Figs. 8 and 9, respectively, for the ground motion records, number 5 and number 13 correspond to 50% summarized IDA curve. As it is seen, applying modification factors on detail coefficient of ground motion records have low effect on the frequency content of the ground motion records. To further illustrate, according to Fig. 8(a) and Table 4, the modification factors for the generated ground motion record number 5 at the fourth level of DWT is 0.273, therefore, the response spectrum in the periodic interval [0.32 0.64] s correspond to the fourth level of DWT is decreased.

According to Luco and Bazzurro (2007), the frequency content of the selected ground motion records to do non-linear dynamic analysis and IDA should reflect the seismic hazard of the site. Although, the frequency content of the generated ground motion records is modified, but the change is negligible while they generally estimate the summarized IDA curves achieved by original ground motion records.

In other to investigate the efficiency of BOA to optimize the difference in the results of SDOF system, IDA curves of the ground motion records number 5 and number 13 are drawn for the original and the generated ground motion record for 50% fractile (Fig. 10(a)-(b)). As it can be seen,

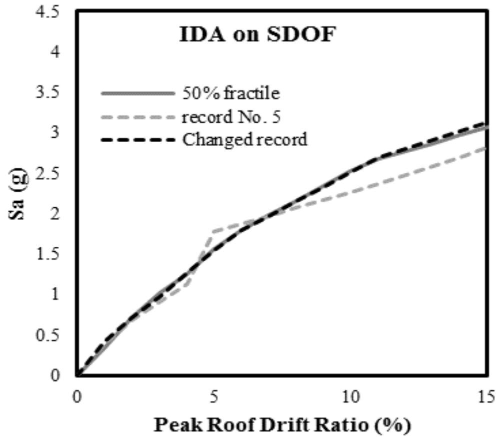

(a) Record No. 5

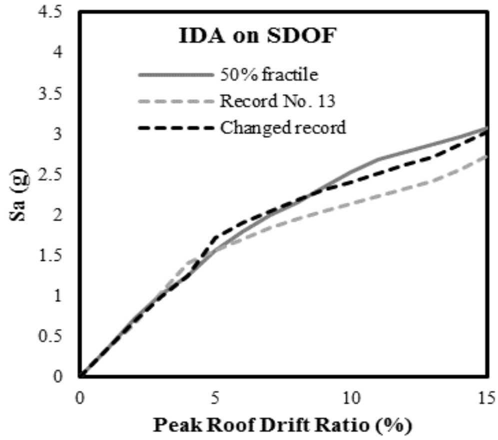

(b) Record No. 13

Fig. 10 Comparison between IDA curves of first ground motion records with and without applying modification factors and 50% IDA fractile on SDOF system

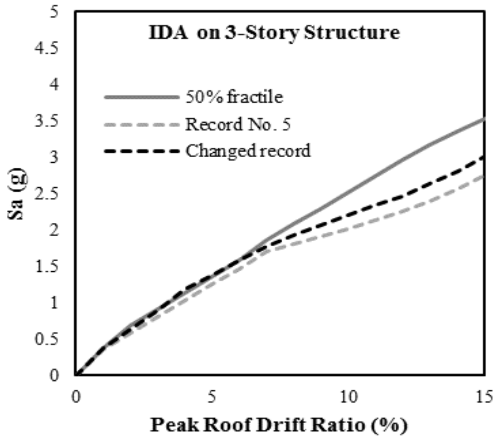

(a) Record No. 5

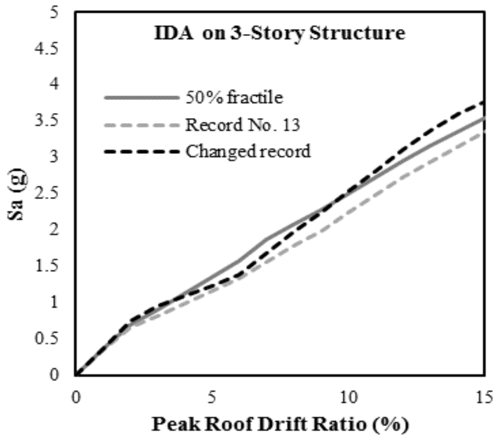

(b) Record No. 13

Fig. 11 Comparison between IDA curves of first ground motion records with and without applying modification factors and 50% IDA fractile on 3-story structure.

after applying the modification factors, the difference of IDA curves for the original, and the generated ground motion record number 5 and number 13 is remarkably changed from 8.8 to 1.4, and 8.6 to 2.7 percentage, respectively.

6. Case study

To sum up, the feasibility of proposed method, the original and the generated ground motion records are implemented to run IDA for the 3-story structure and to compare the summarized IDA curves (Fig. 11(a)-(b)).

According to Fig. 11 the difference of IDA curves for the original, and the generated ground motion record number 5 and number 13 is changed from 18 to 11.3, and 9.9 to 5.7 percentage, respectively. The more difference comparing to SDOF system can be attributed to the contribution of higher modes in the actual response of multi-degree of freedom structures; nonetheless, an improvement in the accuracy of the estimated summarized IDA curve for the 3-storys structure is obvious. In other words, the proposed method has an inherent restriction to be used for structures that their response to ground motion excitation is dominated by the first mode of vibration.

The appropriate number of the selected ground motions records to estimate the summarized IDA curves should be chosen meticulously. The more ground motion record's number, the more analysis time, while having more accuracy. The total IDA difference (Eq. (8)) for a various number of selected ground motion records were considered as a determining criterion, and as a general rule, choosing three records yielded to satisfying results.

Fig. 12(a)-(b) shows the IDA difference of the peak roof drift and maximum inter-story drift ratio, respectively, for a different number of selected ground motion record (from 1 to 5). According to Fig. 12 increasing the number of selected ground motion record can almost decrease the IDA difference value for estimated summarized IDA curve of the 3-story structure. Also, it can be seen, selecting 3 ground motion records have acceptable accuracy and the lowest time of analysis for estimating the summarized IDA curves.

Fig. 13(a)-(b) shows the summarized IDA curves of the 3-story and the average IDA curves, which are determined based on the 3 generated ground motion records. Fig. 13(a) and 13(b) show IDA curves based on the peak roof drift and maximum inter-story drift ratio, respectively.

According to Fig. 13, there is good compatibility

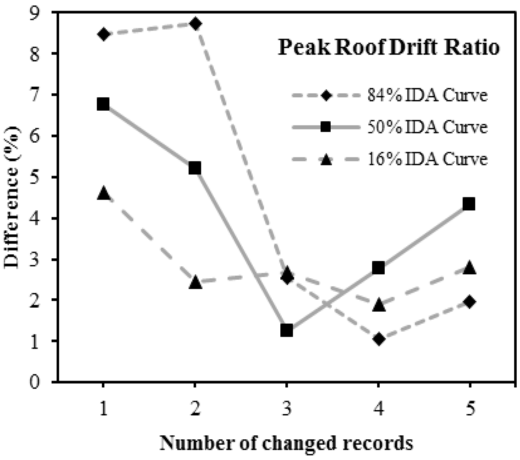

(a) The difference for IDA curves based on peak roof drift ratio

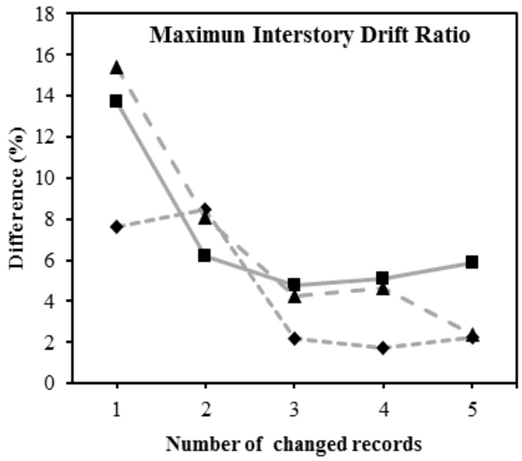

(b) The difference for IDA curves based on maximum inter-story drift ratio

Fig. 12 IDA difference values calculated from Eq. (8) for estimation the summarized IDA curves of 3-story structure for a different number of selected ground motion record

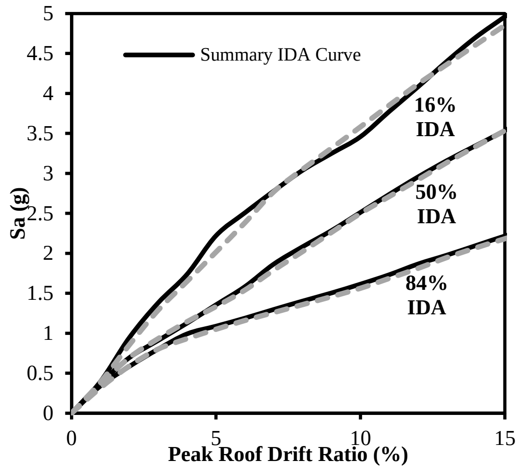

(a) IDA curves based on peak roof drift ratio

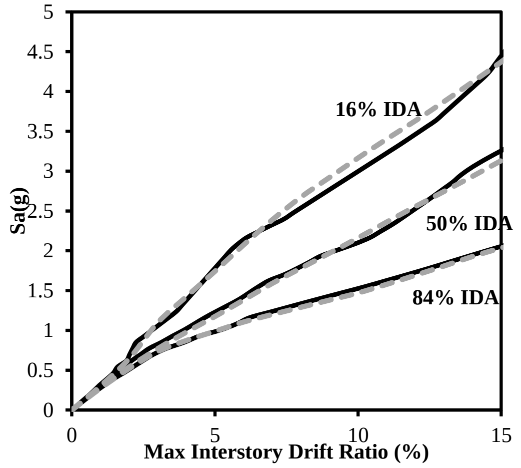

(b) IDA curves based on maximum inter-story drift ratio

Fig. 13 Comparison of average IDA curves of 3 generated ground motion records and summarized IDA curve of 3-story structure

Table 5 Number of time history analysis and computational time

Analysis method	Conventional IDA	Proposed (for each summarized IDA curve)
Number of time history analysis on 3-story structure	240	36
Time for running the analysis (min)	612	143

between the estimated summarized IDA curve and the summarized IDA curve of the 3-story structure. Therefore, by selecting 3 generated ground motion records, the difference of estimating summarized IDA curve is below the acceptable level of 10% and doesn't require considering a further number of ground motion records.

Since the utilized procedure was extended from SDOF model, which can predict only the peak roof drift ratio, the IDA difference for the maximum inter-story drift ratio is higher than the IDA difference determined for the peak-roof drift ratio (Fig. 12).

The efficiency of the procedure depends on the ability of the SDOF system to estimate the DM of the 3-story structure. For buildings, which are not first mode dominant or the structure possesses several non-linear parameters, using the equivalent SDOF system based on the first mode of the structure may not be an appropriate approach. Considering more structural mode may lead a good accuracy for those kinds of structures. Besides, a larger number of (more than 3) generated ground motion records may require for the estimation of the summarized IDA curves of the structure. Also, the non-linear dynamic result can be altered by selecting appropriate hysteretic models for the behavior of SDOF.

The time required for performing the step 1 to 7 of the proposed method is approximately the same as the time required for IDA by one ground motion record (record number 2) from Table 2. In Table 5 the number of time history analysis on 3-story structure and run time for each normal and proposed analysis method are presented. According to Table 5, the procedure reduces the time of the estimation for each summarized IDA curve to 23% of the original IDA on the 3-story structure with all ground motion record from Table 2.

7. Conclusions

In this paper, the frequency content of selected ground motion records is modified by using the discrete wavelet transform and bees optimization algorithm to save computational cost and have an acceptable estimation of the summarized IDA curve of a first-mode-dominated structure. To perform this method, an equivalent SDOF system of the target structure is idealized based on pushover analysis. Then, an appropriate hysteretic model representing the structural behavior of main structure is adapted to SDOF system. The response of SDOF is used as a criterion to select the appropriate ground motions which have lower IDA difference comparing the summarized IDA curve of SDOF system. The frequency content of selected ground motion records is modified by means of bees optimization algorithm to fit better to the summarized IDA curve of SDOF system. Later on, the generated ground motion records are used to estimate the summarized IDA curve of the main structure.

To illustrate the proposed method, a case study of a 3-story steel special moment frame is investigated. For each summarized IDA curve 3 ground motion records were selected based on Eq. (8). Using the selected 3 generated ground motion records leaded to an estimation of the target summarized IDA curves with high accuracy. Also, in the case of using 3 generated ground motion records, the estimation IDA difference (Eq. (8)) of summarized IDA curves are in acceptable range for practical application and there is no need to consider additional generated ground motion records. To sum up, the proposed method significantly reduces the computational cost (almost 23% normal procedure) for the estimation of the summarized IDA curve by decreasing the number of required ground motion records compared to the exact IDA procedure.

References

Amini, F., Khanmohamadi Hazaveh, N. and Abdolahi Rad, A. (2013), “Wavelet PSO-based LQR algorithm for optimal structural control using active tuned mass dampers”, *Comput. Aid. Civil Infrastr. Eng.*, **28**(7), 542-57.

Azarbakht, A. and Dolšek, M. (2007), “Prediction of the median IDA curve by employing a limited number of ground motion records”, *Earthq. Eng. Struct. Dyn*., **36**, 2401-2421.

Azarbakht, A. and Dolšek, M. (2011), “Progressive incremental dynamic analysis for first-mode dominated structures”, *J. Struct. Eng*., **137**, 445-455.

Dolšek, M. and Fajfar, P. (2005), “Simplified non-linear seismic analysis of infilled reinforced concrete frames”, *Earthq. Eng. Struct. Dyn*., **34**, 49-66.

Dorigo, M., Maniezzo, V. and Colorni, A. (1996), “The ant system: optimization by a colony of cooperating agents”, *IEEE Tran. Syst. Man. Cybern.*, **B26**(1), 29-41.

Dremin, I.M. (2005), “Wavelets: Mathematics and applications”, *Phys. Atomic. Nucl.*, **68**(3), 508-520.

Eberhart, R.C. and Kennedy, J. (1995), “A new optimizer using particle swarm theory”, *Proceedings of the Sixth International Symposium on Micro Machine and Human Science*, Nagoya, Japan.

Eghbali, M., Ghodrati Amiri, G. and Raissi Dehkordi, M. (2015), “Evaluation of modified nonlinear dynamic and static analyses for seismic behavior of steel moment-resisting frames”, *J. Vibroeng.*, **17**(8), 4313-4324.

Fajfar, P. (1999), “Capacity spectrum method based on inelastic demand spectra”, *Earthq. Eng. Struct. Dyn.*, **28**(9), 979-993.

Fan, Z., Feng, X. and Zhou, J. (2013), “A novel transmissibility concept based on wavelet transform for structural damage detection”, *Smart Struct. Syst.*, **12**(3-4), 291-308.

Ghodrati Amiri, G. and Namiranian, P. (2013), “Hybrid artificial neural networks based on ACO-Rprop for generating multiple spectrum-compatible artificial earthquake records for specified site geology”, *Int. J. Optim. Civil Eng.*, **3**(1), 179-207.

Ghodrati Amiri, G., Abdolahi Rad, A. and Khanmohamadi Hazaveh, N. (2014), “Wavelet-based method for generating nonstationary artificial pulse-like near-fault ground motions”, *Comput. Aid. Civil Infrastr. Eng.*, **29**, 758-770.

Ghodrati Amiri, G., Abdolahi Rad, A., Aghajari, S. and Khanmohamadi Hazaveh, N. (2012), “Generation of near-field artificial ground motions compatible with median-predicted spectra using PSO-based neural network and wavelet analysis”, *Comput. Aid. Civil Infrastr. Eng.*, **27**, 711-30.

Ghodrati Amiri, G., Shahjouei, A., Saadat, S. and Ajallooeian, M. (2011), “Hybrid evolutionary-neural network approach in generation of artificial accelerograms using principal component analysis and wavelet-packet transform”, *J. Earthq. Eng.*, **15**, 50-76.

Gupta, A. and Krawinkler, H. (1999), “Seismic demands for performance evaluation of steel moment resisting frame structures (SAC Task 5.4.3)”, Report No. 132, John A. Blume Earthquake Engineering Center, Stanford University, Stanford, CA.

Han, S.W. and Chopra, A.K. (2006), “Approximate incremental dynamic analysis using the modal pushover analysis procedure”, *Earthq. Eng. Struct. Dyn*., **35**(15), 1853-1873.

Hancock, J., Watson-Lamprey, J., Abrahamson, N.A., Bommer, J., Markatis, A., Mccoy, E. and Mendis, R. (2006), “An improved method of matching response spectra of recorded earthquake ground motion using wavelets”, *J. Earthq. Eng.*, **10**, 67-89.

Holland, J.H. (1975), “Adaptation in natural and artificial systems”, University of Michigan Press, Ann Arbor.

Ibarra, L.F., Ricardo, A. and Krawinkler, H. (2005), “Hysteretic models that incorporate strength and stiffness deterioration”, *Earthq. Eng. Struct. Dyn*., **34**, 1489-1511.

Kim, H. and Adeli, H. (2005), “Hybrid control of smart structures using a novel wavelet-based algorithm”, *Comput. Aid. Civil Infrastr. Eng.*, **20**(1), 7-22.

Luco, N. and Bazzurro, P. (2007), “Does amplitude Scaling og ground motion records result in biased nonlinear structure drift responses”, *Earthq. Eng. Struct. Dyn.*, **36**(13), 1813-1835.

Mazzoni, S., McKenna, F., Scott, M.H. and Fenves, G.L. (2007), “OpenSees Command Language Manual”, Pacific Earthquake Engineering Research Center, University of California, Berkeley.

Mofid, M., Zarfam, P. and Fard B.R. (2005), “On the modal incremental dynamic analysis”, *Struct. Des. Tall Spec. Build.*, **14**, 315-329.

Ovanesova, A.V. and Suárez, L.E. (2004), “Applications of wavelet transforms to damage detection in frame structures”, *Eng. Struct.*, **26**, 39-49.

Peruš, I., Klinc, R., Dolenc, M. and Dolšek, M. (2015), “Innovative computational environment for fast and acuurate prediction of approximate IDA curves”, *Comput. Meth. Appl. Sci.*, **30**, 259-272.

Pham, D.T., Ghanbarzadeh, A., Koc, E., Otri, S., Rahim, S. and Zaidi, M. (2005), "The bees algorithm", Technical Note, Manufacturing Engineering Centre, Cardiff University, UK.

Politis, N. (2002) "Advanced time-frequency analysis applications in earthquake engineering", *Student Research Accomplishment, 2000-2003*, Multidisciplinary Center for Earthquake Engineering Research, Buffalo, New York.

Sirca, G.F. and Adeli, H. (2004), "A Neural Netwok-Wavelet Model for Generating Artificial Ground motion records", *Int. J. Wavel. Multiresol. Inform. Pr.*, **2**(3), 217-235.

Solís, M., Algaba, M. and Galvín, P. (2013), "Continuous wavelet analysis of mode shapes differences for damage detection", *Mech. Syst. Signal Pr.*, **40**(2), 645-666

Tibaduiza, D.A., Torres-Arredondo, M.A., Mujica, L.E., Rodellar, J. and Fritzen C.P. (2013) "A study of two unsupervised data driven statistical methodologies for detecting and classifying damages in structural health monitoring", *Mech. Syst. Signal Pr.*, **41**(1-2), 467-484.

Vamvatsikos, D. and Cornell, C.A. (2002), "Incremental dynamic analysis", *Earthq. Eng. Struct. Dyn.*, **31**, 491-514.

Vamvatsikos, D. and Cornell, C.A. (2004), "Applied Incremental Dynamic Analysis", *Earthq. Spectra*, **20**(2), 523-553.

Vamvatsikos, D. and Cornell, C.A. (2005), "Direct estimation of seismic demand and capacity of multi-degree of freedom systems through incremental dynamic analysis of single degree of freedom approximation", *J. Struct. Eng.*, ASCE, **131**(4), 589-599.

Vamvatsikos, D. and Cornell, C.A. (2006), "Direct estimation of the seismic demand and capacity of oscillators with multi-linear static pushovers through IDA", *Earthq. Eng. Struct. Dyn.*, **35**, 1097-1117.

Xiang, J. and Liang, M. (2012), "Wavelet-based detection of beam cracks using modal shape and frequency measurements", *Comput. Aid. Civil Infrastr. Eng.*, **27**(6), 439-54.

Zarfam, P. and Mofid, M. (2011), "On the modal incremental dynamic analysis of reinforced concrete structures, using a trilinear idealization model", *Eng. Struct.*, **33**, 1117-1122.

KT